^{10}Be age control of glaciation in the Beartooth Mountains, USA from the latest Pleistocene through the Holocene

Aaron M. Barth[1], Elizabeth G. Ceperley[2], Claire Vavrus[2], Shaun A. Marcott[2], Jeremy D. Shakun[3], Marc W. Caffee[4,5]

[1]Department of Geology, Rowan University, Glassboro, NJ, USA

[2]Department of Geoscience, University of Wisconsin – Madison, Madison, WI, USA

[3]Department of Earth and Environmental Sciences, Boston College, Chestnut Hill, MA, USA

[4]Department of Physics and Astronomy, Purdue University, West Lafayette, IN, USA

[5]Department of Earth, Atmospheric, and Planetary Sciences, Purdue University, West Lafayette, IN, USA

correspondence to: Aaron M. Barth (bartha@rowan.edu)

Abstract. Alpine glaciers in the western United States are often associated with late-Holocene Little Ice Age (LIA) advances. Yet, recent studies have shown many of these glacial landforms are remnants of latest-Pleistocene retreat with only the most cirque-proximal moraines preserving LIA activity. Additionally, the timing and magnitude of glacial advances during the Neoglacial-LIA interval remains uncertain with presumed maximum extents occurring during the LIA driven by lower Northern Hemisphere insolation levels. Here we present ^{10}Be surface exposure ages from a glacial valley in the Beartooth Mountains of Montana and Wyoming, United States. These new data constrain the presence of the glacier within 2-3 km of the cirque headwalls by the end of the Pleistocene with implications for large-scale retreat after the Last Glacial Maximum. Cirque moraines from two glaciers within the valley preserve a late-Holocene readvance with one reaching its maximum prior to 2.1 ± 0.2 ka and the other 0.2 ± 0.1 ka. Age variability among the moraines demonstrates that not all glaciers were largest during the LIA and presents the possibility of regional climate dynamics controlling glacial mass balance.

1 Introduction

Glacier retreat is one of the clearest indicators of the cryosphere's response to recent global warming. Photographic and satellite imagery of reductions in global glacier extent from the past century document widespread retreat (Bolch, 2007; Catania et al., 2018). Within the last two decades alone, the rate of ice loss from mountain glaciers has doubled (Hugonnet et al., 2021). However, analysis of glacier sensitivity to climate change using the instrumental record is limited by data which only goes back decades (Braumann et al., 2020). We are therefore reliant on geologic records of past glacier activity to determine the influence of anthropogenic warming on glacier mass balance relative to natural variability. In the early Holocene, glaciers within the western United States (U.S.) and Canada were at minimum lengths, similar to modern, with peak Northern Hemisphere (NH) summer insolation values contributing to the retreat (Solomina et al., 2015). Reactivation of glaciation after 6 ka ("Neoglacial") occurred as glaciers advanced to their greatest Holocene extent (Porter and Denton, 1967; Solomina et al., 2016, 2015). Relative to the last glacial period, the Holocene was considerably more stable in terms of its climate variability. However, variable timing of

glacier maximum extent throughout the Neoglacial suggests other mechanisms controlled glacier size besides NH insolation. Well-dated records of late-Holocene glaciation are therefore required to accurately assess forcing mechanisms for the Neoglacial.

Many mountain ranges of the western U.S. remained below the southern reaches of the Laurentide Ice Sheet during the Last Glacial Maximum (LGM, 26 – 19 ka; Clark et al., 2009) where numerous alpine glaciers and icecaps nucleated (Laabs et al., 2020). LGM glacial positions are recorded as down valley moraines extending as much as 50 km from the cirques while younger, high-elevation glacial landforms are preserved within 1-2 km of the headwall (Davis, 1988; Davis et al., 2009). These younger glacial deposits were originally thought to record Neoglaciation, but recent dating concluded that many of these landforms across the western U.S. are in fact remnants of latest Pleistocene and earliest Holocene glaciation (Marcott et al., 2019). The questions then arise: what is the record of late Holocene glaciation in the western U.S., if any exists at all? What does it tell us about the response of mountain glaciers to climatic forcings throughout the Holocene, and were they sufficient to permit glacial regrowth?

Here we present ^{10}Be exposure ages from high-elevation glacial landforms in the Beartooth Mountains of Montana (MT) and Wyoming (WY) to determine the timing of glaciation in this sector of the western U.S. Together with previously published ages on downvalley LGM moraines, this new chronology sheds light on the rate and magnitude of glacier retreat during the last deglaciation as well as potential Neoglacial regrowth during the late Holocene.

2 Geologic and geomorphic background

The Beartooth Mountain range extends from southwestern MT into northern WY and is a broadly arcuate mountain range reaching ~30 km at its widest. At its base, the Mill Creek-Stillwater Fault Zone separates the northern foothills of the Beartooth Mountains from the Great Plains (Fig. 1; Bevan, 1923; Montgomery and Lytwyn, 1984) with ~1800 m relief between the Plains (~1800 m asl) and the highest elevations in the mountain range (>3600 m asl). High plateaus have been dissected by fluvial and glacial erosion. Numerous cirques and northward-oriented glacial valleys are present within the Beartooths, whereas the Absaroka Range to the south exhibits more south- and eastward-oriented glacial valleys. The eastern portion of the mountain range is predominantly Archean quartz-rich granitic gneisses and migmatites with inclusions of metasedimentary and metaigneous rocks (Van Gosen et al., 2000). Coarse-crystalline pegmatitic dikes are common throughout the region (Bevan, 1923).

Glacial landforms in the mountain range record multiple phases of glaciation, including the Bull Lake (Marine Isotope Stage (MIS) 6), and Pinedale (MIS 2) glaciations. Bull Lake glaciation within the northeast sector of the Beartooths is recorded as remnant outwash terraces of higher elevation to those of the younger Pinedale terraces (Ballard, 1976). Morainal evidence, however, is sparse for Bull Lake glacier limits and is suggestive of similar, or lesser, glacial extents to Pinedale advances (Licciardi and Pierce, 2018). During the last glaciation, high-elevation ice flowed southward to the Yellowstone Plateau where it coalesced with similar glaciers from the surrounding mountains forming the Yellowstone ice cap, which acted as an ice divide at the LGM (Licciardi and Pierce, 2018, 2008). Numerous, long (>20 km) glacial valleys are present along the periphery of the Greater Yellowstone Glacial System (GYGS), including those of the northern Beartooths. Glacial deposits including erratics, moraines, and outwash

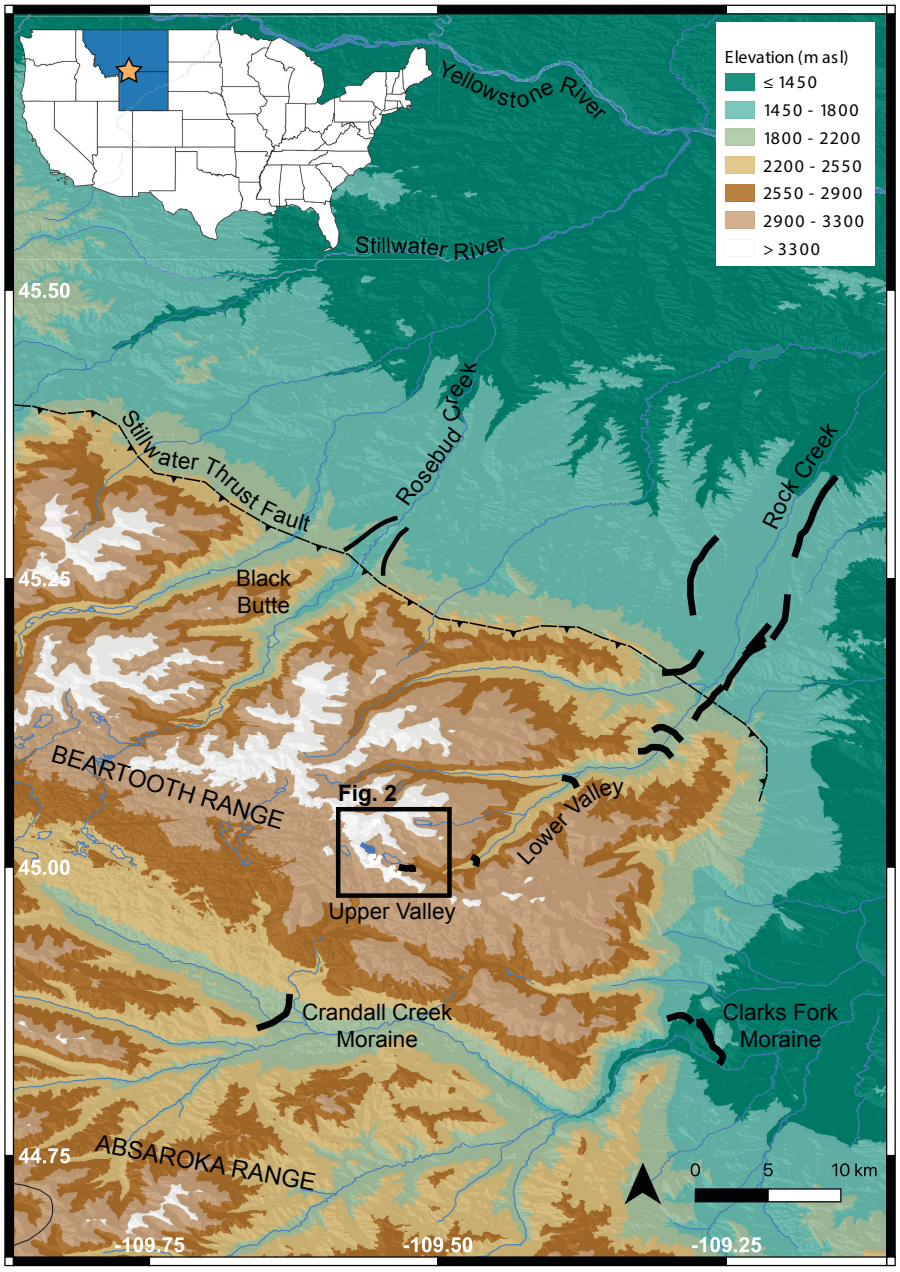

Figure 1 – Regional Map – Map of the Beartooth Mountain range in Montana and Wyoming, United States. Brown colors indicate higher elevation, and green colors lower elevation. Solid black lines show the location of prominent moraines including those mapped by Graf (1971) in the Rock Creek drainage. Inset map shows the location of Montana (MT) and Wyoming (WY) highlighted in blue with approximate location of our study area indicated by the star. Elevation data from the U.S. Geological Survey 3D Elevation Program (U.S. Geological Survey, 20171130, USGS 13 arc-second n46w110 1 x 1 degree: U.S. Geological Survey).

terraces are common within these valleys and provide abundant geologic evidence of past glacial activity from the LGM and deglaciation. Higher in the valleys, proximal to cirque headwalls, additional glacial evidence is preserved as sharp-crested moraines, rock glaciers, and protalus lobes (Davis, 1988; Graf, 1971). Most features are mapped within 1-2 km from cirque headwalls and may represent multiple phases of glaciation (Davis, 1988). Based on geomorphologic characteristics, Graf (1971) identified such features in the Beartooths as two periods of late-Holocene

glaciation. However, geochronologic data are limited by relative-age methods and their associated uncertainties (Davis, 1988).

The Rock Creek drainage, a ~25 km long glacial valley, exits from the northeast corner of the Beartooth Range with associated cirque valleys, including Glacier Lake Valley (study area), located along the border between MT and WY and just north of Yellowstone National Park (Fig. 1 & 2). The lower portion of this drainage (herein referred to as the Lower Valley) is fed by five higher-elevation glacial cirques, trends southwest-northeast, and drains into the town of Red Lodge, MT. Sets of lateral moraines extend north from the valley mouth and bound the town on the eastern and western sides. The lateral moraines define an elongate and relatively narrow former glacier, and they are similar in morphology and size to moraines in valleys 25 km to the west beneath Black Butte. Outboard of the moraines, there are fluvially-modified hills unaffected by glacial activity, while outwash sediments between the lateral moraines suggest extensive meltwater drainage from the Lower Valley. A terminal moraine for this glacier is not preserved, likely due to erosion from meltwater flowing north to the Yellowstone River (Fig. 1). Graf (1971) mapped five moraines within the Lower Valley, although preservation is patchy, including stream breaches ranging from 70 m wide to as wide as the valley floor in some cases. Steep sloped, rocky walls define the valley width, which averages 1.5 to 2.0 km at its widest and narrows further upvalley. Occasional large (>1 m) boulders along the valley floor exhibit glacially-faceted surfaces and striations. The Lower Valley is gently sloped, gaining only 800 m of elevation from the Great Plains over 25 km.

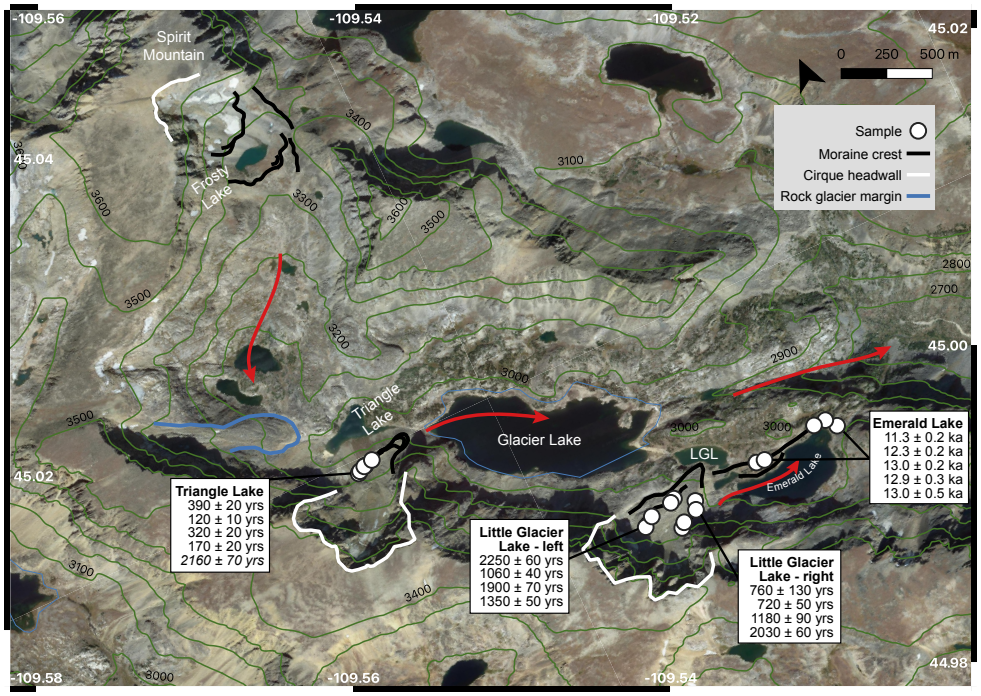

Figure 2 - Glacier Lake Valley map - Map of the study area highlighting the names of important locations discussed in the paper. White lines indicate the cirque headwalls. Solid black lines show the location of moraines. White circles indicate the locations of surface exposure samples with their ages contained in the respective boxes. Statistically identified outliers are italicized. LGL = Little Glacier Lake. Red arrows indicate generalized ice flow direction. Elevation data from the U.S. Geological Survey 3D Elevation Program (U.S. Geological Survey, 20171130, USGS 13 arc-second n46w110 1 x 1 degree: U.S. Geological Survey).

There is a steep, 400 m-high transition from the Lower Valley to Glacier Lake valley (herein referred to as the Upper Valley), capped by an exposed, glacially-abraded, bedrock lip. Four lakes are located between 2960-2970 m asl within the Upper Valley (from east to west): Emerald Lake, Little Glacier Lake, Glacier Lake, and Triangle Lake (Fig. 2). Two of the lakes, Emerald Lake and Little Glacier Lake, are bounded by the bedrock lip to the north. To the south, Emerald Lake is bounded by an exposed bedrock cliff while Little Glacier Lake by a bouldery moraine. A curved boulder-covered moraine exists in the gentle topography between the two lakes (referred to as the Emerald Lake moraine) and is the stratigraphically oldest moraine in the Upper Valley (Graf, 1971). The Emerald Lake moraine has a subdued cross-profile suggestive of moraine degradation over time from the removal of finer grained material from the peak to the flanks (Putkonen et al., 2008; Sortor, 2022). The location and size of Glacier Lake is controlled by steep rocky walls to the north and south with colluvial fans along the base of the southern wall. Two bedrock knobs separate Glacier Lake from Triangle Lake to the west, with morainal deposits restricting water flow between the two (Graf, 1971). To the northwest of Triangle Lake, a rounded and smoothed bedrock exposure increases elevation as the valley changes orientation to north-south and gains another ~450 m of elevation. A small cirque below the peak of Spirit Mountain (3744 m asl) contains a lake, Frosty Lake, and two moraines along both the down- and upvalley shores. The downvalley moraine is low-relief, bouldery, and rests on the cirque lip. The upvalley moraine is 50 m tall, sharp-crested, within 25 m of modern ice, and morphologically similar to the moraine at Triangle Lake. No prominent moraines are present between Triangle Lake and those at Frosty Lake.

The cirque near Little Glacier Lake preserves two moraines with an additional moraine in the cirque near Triangle Lake (Fig. 2). The moraines around Little Glacier Lake have high-angle lateral slopes of large (>1 m) angular boulders mixed with coarse to fine sands and all grain sizes in between (Fig. 3). The toe of the moraine is lower-relief (15 m), dominated by boulders, and rests along the southern shore of Little Glacier Lake. The left-lateral moraine rests on a bedrock outcrop at 3022 m asl (Fig. 3B). Ribbed crests of boulder deposits are found inboard of the left lateral moraine and maintain a similar elevation throughout. Between the lateral moraines, the surface elevation remains fairly consistent, with drastic changes in slope only along the distal sides of the moraines. While the moraine crests are easily defined, abundant boulder debris coverage within the moraine limits is suggestive of rock glacier activity or rockfall from over-steepened cliff faces. Small patches of modern ice are visible near the headwall but are covered in debris further down slope.

A steep-sloped moraine is found along the southern shore of Triangle Lake, ~1.2 km north of a cirque headwall containing a small (~0.1 km^2), debris-covered glacier. The moraine increases in relief from 35 m near the terminus to 80 m along the lateral aspects and contains abundant coarse sands and gravels among numerous angular boulders (>0.4 m in height). The peak of the moraine is narrow and exhibits minimal deflation, yet occasional patches of grass and soil suggest the surficial deposits are not recent. From the terminus, the moraine curves to the east to intersect a near-vertical cliff face and is covered with boulders, some up to ~10 m in size. The western aspect of the moraine gains 130 m elevation before encountering a glacially-smoothed bedrock knob. Above the bedrock knob, the moraine continues another 60 m before reaching the glacier.

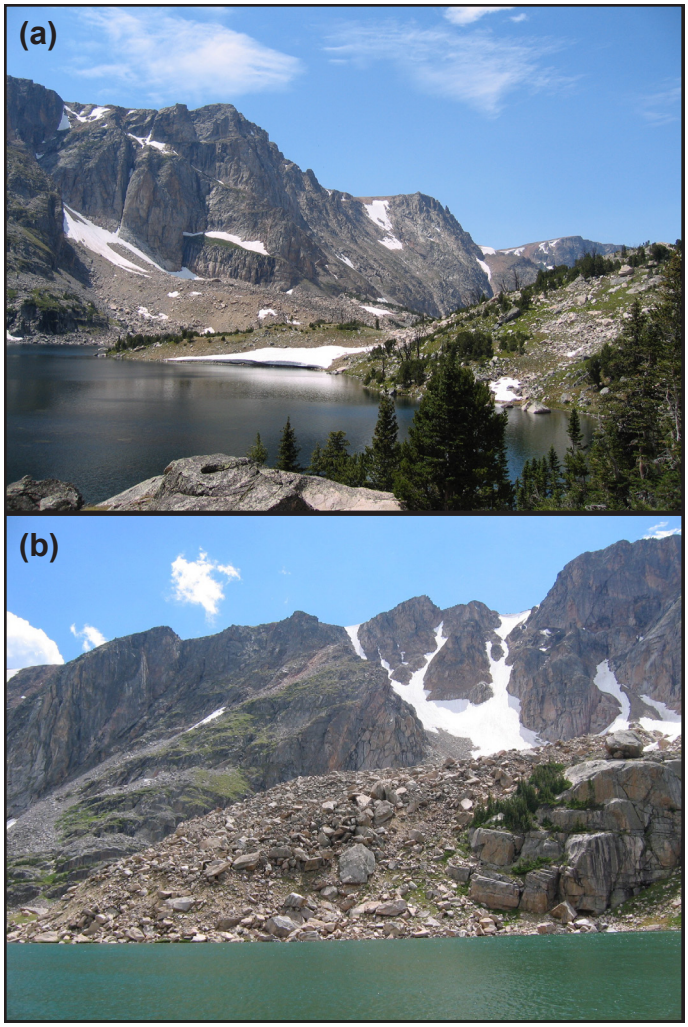

Figure 3 - Beartooth Moraines – (a) Emerald Lake moraine on the left with the Little Glacier Lake moraines in the distance. (b) Toe and left lateral aspect of the Little Glacier Lake moraine and bedrock knob.

3 Methods

To determine the timing of glaciation within Upper Valley, we sampled glacially-deposited boulders for cosmogenic ^{10}Be surface exposure dating from four moraines: one at Triangle Lake, two at Little Glacier Lake, and one at Emerald Lake moraine (Fig. 4). Samples were collected over two field seasons in 2006 (Emerald Lake and Little Glacier Lake) and 2017 (Triangle Lake and Little Glacier Lake) using hammer and tungsten carbide-tipped chisels. Strict sample selection criteria were followed to maximize the accuracy of nuclide accumulation representative of initial deposition by the glacier (Dunai, 2010; Gosse and Phillips, 2001). Boulders selected for sampling exhibited no signs of surficial erosion or pitting that would remove accumulated nuclides. Samples were limited to within the top five centimeters from flat-topped boulders to ensure highest rates of *in-situ* nuclide production. All samples were collected on or near the mapped moraine crest to minimize potential post-depositional movement and associated reduction of nuclide accumulation on the sampled surface. Each boulder was a minimum of 0.4 m in height with an average boulder height of 1.5 m. Potential boulder burial or exhumation is unlikely given boulder height and morphological characteristics of the moraines. Both the Little Glacier Lake and Triangle Lake moraines exhibit little

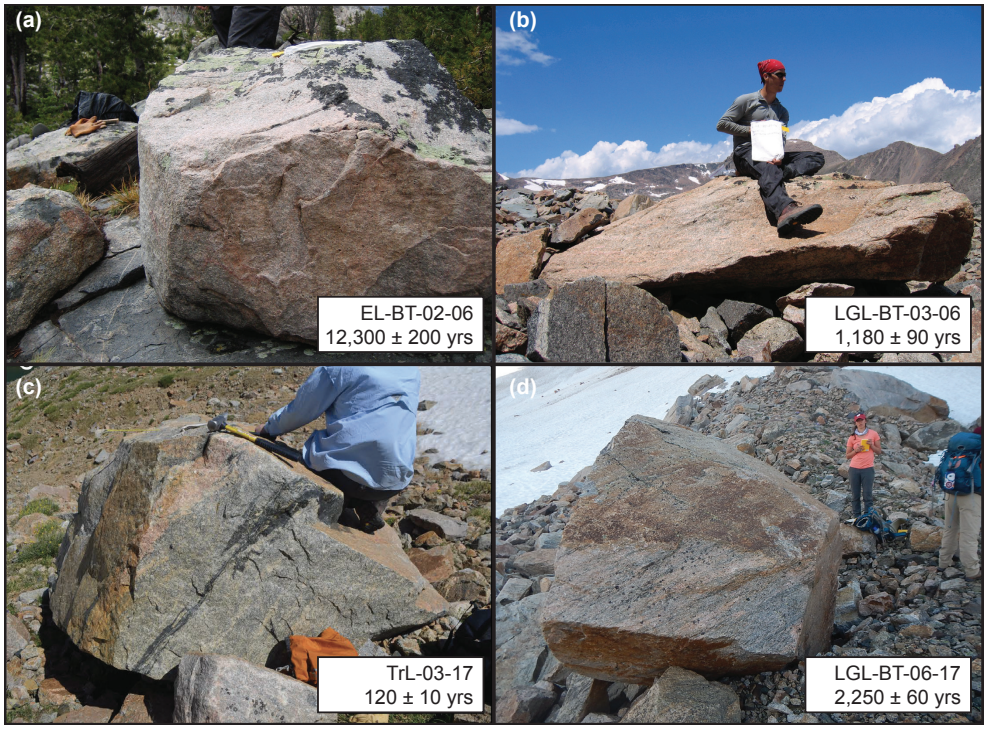

Figure 4 - Sample boulders - Boulders sampled for ^{10}Be surface exposure dating discussed in this project. (a) EL = Emerald Lake. (b,d) LGL = Little Glacier Lake. (c) TrL = Triangle Lake. 1-sigma analytic uncertainty shown for each age.

to no soil cover, which suggests exhumation of boulders from previous cover is unlikely. Latitude, longitude, and elevation were recorded for each sample using a handheld GPS unit and verified using high-resolution DEMs and topographic maps. Surface inclination of each sample was measured using a Brunton compass and topographic shielding was recorded in the field using a clinometer. Shielding scaling factors for each sample were calculated using the CRONUS online Topographic Shielding Calculator (http://stoneage.ice-d.org/math/skyline/skyline_in.html; Balco et al., 2008)

Eighteen samples were collected and processed for ^{10}Be extraction that best represent our selection criteria: five boulders from Emerald Lake, four from the inner Little Glacier Lake moraine, four from the outer Little Glacier Lake moraine, and five from Triangle Lake.

Boulder samples were processed for ^{10}Be extraction at the University of Wisconsin – Madison. The sample processing procedures are adapted from laboratories at Oregon State University, the University of Vermont Cosmogenic Nuclide Laboratory, and the University of New Hampshire (Corbett et al., 2016; Kohl and Nishiizumi, 1992; Licciardi, 2000; Marcott, 2011). Each rock sample was sawed to isolate the top 2-5 cm, crushed and sieved to a 250-710 µm size fraction, magnetically separated, and etched in concentrated HCl and dilute 2% HF/HNO_3 acid solutions. A minimal of three rounds of etching were completed for each sample. Chemical frothing was performed on all non-magnetic grains in order to isolate quartz from feldspar. The remaining quartz grains were isolated using additional HF/HNO_3 etches. Quartz purity was measured by inductively coupled plasma optical emission spectroscopy

(ICP-OES) at the University of Colorado-Boulder Department of Geological Sciences and the University of Wisconsin-Madison Water Science and Engineering Laboratory.

The chemically etched and pure quartz was dissolved in concentrated HF, after an addition of ^{9}Be carrier solution prepared from raw beryl (OSU White standard; ^{9}Be concentration of 251.6 ± 0.9 ppm) (Marcott, 2011). We used anion and cation exchange chromatography to separate Fe, Ti, and Al from Be, and BeOH was precipitated in a pH 8 solution. BeOH gels were converted to BeO by heating to 900-1000ºC with a rapid incinerator, then mixed with Nb powder in quartz crucibles, and packed into stainless steel cathodes for accelerator mass spectrometry (AMS) analysis.

All ^{10}Be/^{9}Be ratios were measured at the Purdue University Rare Isotope Measurement Laboratory (PRIME Lab) and normalized to standard 07KNSTD3110, which has an assumed ^{10}Be/^{9}Be ratio of 2.85 x 10^{12} (Nishiizumi et al., 2007). Sample ratios were corrected using batch-specific blank values that ranged from 2.39 x 10^{-15} to 4.19 x 10^{-15} (n = 3; Table 1). ^{10}Be concentrations presented in Table 1 are corrected from process blanks.

Exposure ages are calculated using version 3.0 of the original online calculator as described in Balco et al. (2008; herein referred to as Version 3.0) and the time-dependent scaling scheme of Lifton et al. (2014; LDSn). We use the ^{10}Be production rate in quartz as determined from Promontory Point, UT (PPT; Lifton et al., 2015) based on proximity to the study site (~700 km) and high confidence in the quality of constraining samples. We note that a recent review of Western U.S. surface exposure ages follows similar methods for recalculating previous published data (Laabs et al., 2020; Licciardi and Pierce, 2018) including those for the GYGS. Wide-ranging rates of surface erosion experienced by glacial erratics are suggested in the literature with rates within the order of 0.0 to 0.1 cm ka^{-1} (Gillespie and Bierman, 1995). Based on the presumed young age of our sampled deposits, we assume surface erosion of the boulders was negligible and therefore do not account for it in our calculations. We follow the procedures outlined in Laabs et al. (2020) and assume the effects of snow cover to be negligible. Individual exposure ages are reported as years before collection date (per Version 3.0 calculations) and with 1-sigma analytical uncertainty. Moraine ages are reported as the arithmetic mean and standard deviation of the boulder ages to present a conservative uncertainty estimate. We note that distribution ages reported using error-weighted mean and uncertainty tend to favor younger exposure ages with lower analytical uncertainty which are more likely to be influenced by geological processes (e.g., surface erosion, post-depositional movement) leading to erroneously young ages (Balco, 2011; Laabs et al., 2020; Licciardi and Pierce, 2008). Outliers are identified using Chauvenet's criterion and interquartile range tests.

4 Results

Resulting ^{10}Be exposure ages demonstrate glaciation within the Upper Valley from the latest Pleistocene and the late Holocene with all ages in stratigraphic order. Five exposure ages from the stratigraphically oldest moraine at Emerald Lake range from 11.3 ± 0.2 to 13.0 ± 0.5 ka (Table 1). Together these samples have a mean age and standard deviation of 12.5 ± 0.7 ka. We note that sample EL-BT-01-06 (11.3 ± 0.2 ka) is 0.9 ka younger than the next youngest sample (EL-BT-02-06; 11.4 ± 0.2 ka), yet cannot be rejected using either of the statistical tests. Removing sample EL-BT-01-06 from the population increases the mean age to 12.8 ka which falls within 1-sigma uncertainty of our reported age and therefore does not change our interpretations.

Samples (n = 4) from the Little Glacier Lake left-lateral moraine yield exposure ages ranging from 1,060 ± 40 yrs to 2,250 ± 60 yrs (Table 1). The Little Glacier Lake right-lateral moraine yielded four exposure ages ranging from 720 ± 50 yrs to 2,030 ± 60 yrs (Table 1). A ~1,300 yr range exists between the oldest and youngest age of the population, however, no samples are rejected using the statistical tests described. The samples in both populations were likely affected by geologic processes.

Five samples from the moraine near Triangle Lake yield exposure ages ranging from 120 ± 10 yrs to 2,160 ± 70 yrs. Sample TrL-07-17 (2,160 ± 70 yrs) is identified as an outlier using both previously mentioned statistical tests. The four remaining samples exhibit an approximate bimodal distribution, but overlap within 2-sigma uncertainty. In our discussion, we interpret the remaining age range of 120 ± 10 yrs to 390 ± 20 yrs.

5 Discussion

5.1 Variable rates of western U.S. glacier retreat from the LGM to the Younger Dryas

During the last deglaciation the timing and rate of retreat of western U.S. glaciers varied spatially (Laabs et al., 2020). Broadly, glacial retreat from LGM margins in the western U.S. began between 22 ka and 18 ka (Shakun et al., 2015; Young et al., 2011). Glaciers from the northern GYGS fall within this window of deglacial onset, with two terminal moraines yielding ^{10}Be exposure ages of 19.8 ± 0.9 ka and 18.2 ± 1.3 ka (Fig. 5; Licciardi and Pierce, 2018). While no geochronologic control exists for the lateral moraines near Red Lodge, a lack of moraines outboard of them suggest they represent a terminal position of the glacier. They are also morphologically similar to other LGM-mapped moraines within the Beartooths (Black Butte; 25 km west of Red Lodge), and are proximal to the dated moraines at Clarks Fork (19.8 ± 0.9 ka) and Pine Creek (18.2 ± 1.3 ka) that are part of the same regional glacial system. Therefore, for our purposes, we assume the age, and therefore the onset of deglaciation, of the Red Lodge moraines to fall within the time window of 22 ka to 18 ka.

Rapid retreat of the Clarks Fork glacier to the Crandall Creek moraine between 19.8 ± 0.9 ka and 18.2 ± 0.8 ka was followed by the construction of multiple recessional moraines as retreat slowed (Licciardi and Pierce, 2018). Initial, rapid retreat of the Clarks Fork glacier is hypothesized to have occurred as migration of the Yellowstone Ice Cap to the southwest created a precipitation shadow for the northeast portion of the GYGS thus affecting glacial mass balance negatively (Licciardi and Pierce, 2018, 2008). Synchronous changes in North American precipitation patterns were affecting glacial mass balance in the central north region of the U.S. (Lora and Ibarra, 2019). These changes in precipitation include migration of the dominant atmospheric jet stream (Lora et al., 2017; Manabe and Broccoli, 1985) and changes in the seasonality of precipitation delivery to certain regions (Lora and Ibarra, 2019). Slower retreat of the Clarks Fork glacier during the Late Pinedale (16-13 ka) is attributed to a reduction of the precipitation shadow in the northeast GYGS as the Yellowstone Ice Cap continued its migration to the southwest (Licciardi and Pierce, 2018). After ~14 ka a more regionally coherent response of glacier retreat occurred in response to warming from increased atmospheric greenhouse gas concentrations (Marcott et al., 2019, 2014; Shakun et al., 2015).

Graf (1971) mapped five moraines within the Lower Valley between our prescribed LGM moraines and the Upper Valley which mark the location of the glacier as it retreated from its terminal position (Fig. 1). Based on geomorphological evidence such as distance regression, soil development, and shape index, the two furthest down

Table 1 - Sample data and ^{10}Be concentrations										
Sample name	Latitude (DD)	Longitude (DD)	Elevation (m)	Thickness (cm)	Shielding	Date	Conc. (atoms g^{-1})	Conc. unc. (atoms g^{-1})	Age (yrs)	Moraine age (yrs)
Triangle Lake[a]										
TrL-02-17	45.00993	-109.55342	3064	2	0.937	2017	17996	992	390 ± 20	
TrL-03-17	45.01003	-109.55327	3056	2	0.939	2017	5229	560	120 ± 10	
TrL-05-17	45.01023	-109.55276	3049	5	0.939	2017	14573	850	320 ± 20	
TrL-06-17	45.01021	-109.55286	3049	4	0.939	2017	7370	647	170 ± 20	
TrL-07-17	45.01039	-109.55219	3058	2	0.939	2017	84217	2632	2160 ± 70	
Little Glacier Lake - left lateral[a]										
LGL-BT-04-17	44.99907	-109.53428	3023	2	0.951	2017	53327	1863	1350 ± 50	
LGL-BT-05-17	44.9989	-109.5346	3045	2	0.96	2017	74396	2668	1900 ± 70	
LGL-BT-06-17	44.9981	-109.5369	3057	2	0.909	2017	85516	2366	2250 ± 60	
LGL-BT-07-17	44.9986	-109.5362	3060	2	0.938	2017	45089	1664	1060 ± 40	
Little Glacier Lake - right lateral[b]										
LGL-BT-01-06	44.99698	-109.53462	3094	2	0.891	2006	33396	5584	760 ± 130	
LGL-BT-02-06	44.99728	-109.53433	3075	2	0.891	2006	31674	2156	720 ± 50	
LGL-BT-03-06	44.99772	-109.53322	3057	2	0.935	2006	47683	3620	1180 ± 90	
LGL-BT-02-17	44.9983	-109.533	3042	2	0.981	2017	81645	2443	2030 ± 60	
Emerald Lake[b]										12500 ± 700
EL-BT-01-06	44.99887	-109.52185	2999	2	0.969	2006	477331	8107	11300 ± 200	
EL-BT-02-06	44.99957	-109.52243	2993	2	0.989	2006	517609	8749	12300 ± 200	
EL-BT-03-06	44.99957	-109.5233	2990	2	0.989	2006	537278	9494	13000 ± 200	
EL-BT-06-06	44.99892	-109.52802	2989	2	0.977	2006	528085	14047	12900 ± 300	
EL-BT-07-06	44.99885	-109.52743	2991	2	0.977	2006	533612	21843	13000 ± 500	
Blanks										
Blank-004	-	-	-	-	-	-	54395	10291	-	
Blank-005	-	-	-	-	-	-	37559	8405	-	
Blank-024	-	-	-	-	-	-	30634	5901	-	
[a]Samples that used Blank-024 in calculations										
[b]Samples that used Blank-004 and Blank-005 in calculations										

valley moraines were associated with Bull Lake glaciation and the three more upvalley moraines as Pinedale terminal moraines. Furthermore, Graf (1971) assigned the Pinedale moraines correlative ages with other Western U.S. deposits ranging from 23.0 ka for the outermost to 11.5 ka for a moraine found near the steep transition from Lower to Upper Valley. However, based on the reasons described above, we argue all deposits within the Lower Valley are more likely representative of post-LGM deglaciation similar to proximal glacier valleys within the GYGS (Laabs et al., 2020; Licciardi and Pierce, 2018, 2008). Additionally, the age of glacial retreat we obtained for the Emerald Lake moraine (12.5 ± 0.7 ka) inboard from the Graf (1971) 11.5 ka Lower Valley moraine suggests stabilization of the glacial prior to 12.5 ± 0.7 ka and is therefore in stratigraphic disagreement with this assigned age. As such, the Lower Valley deposits must be older than 12.5 ± 0.7 ka, and represent a period of glaciation between the end of the LGM (22 ka to 18 ka) and formation of the Emerald Lake moraine (Fig. 5).

The five Lower Valley moraines between Red Lodge and the Upper Valley suggest multiple periods of stagnation or glacial readvance during the last deglaciation. A lack of numerical age control limits our ability to assess the rate and timing of retreat within the Lower Valley. However, stratigraphic relationships of the moraines along with chronologic control higher in the valley permit a certain amount of bookending.

The Emerald Lake moraine marks the next geochronologically-constrained position of the glacier following the LGM. Using the time window of 22 ka to 18 ka for the onset of LGM deglaciation in Red Lodge and the age of the Emerald Lake moraine as limiting ages we determined a maximum and minimum mean retreat rate of the glacier of 4.9 m/yr (18.0 – 12.5 ka) and 2.8 m/yr (22.0 – 11.6 ka), respectively. These values are lower than those recorded for the nearby Clarks Fork glacier, which lost 75-90% of its LGM length between 19.8 ± 0.9 ka and 18.2 ± 0.8 ka at a mean retreat rate of 28.0 m/yr (Licciardi and Pierce, 2018).

We hypothesize that retreat of the Rock Creek glacier from its LGM limit began later in the window of LGM retreat (22 to 18 ka) similar to the Pine Creek moraine (18.2 ± 1.3 ka). After which the Rock Creek glacier experienced

slower retreat similar to that of the Clarks Fork glacier after abandoning the Crandall Creek moraine (18.2 ± 0.8 ka), thus allowing for the formation of morainal features within the Lower Valley. Eventually the glacier left the Lower Valley in response to rising atmospheric greenhouse gases.

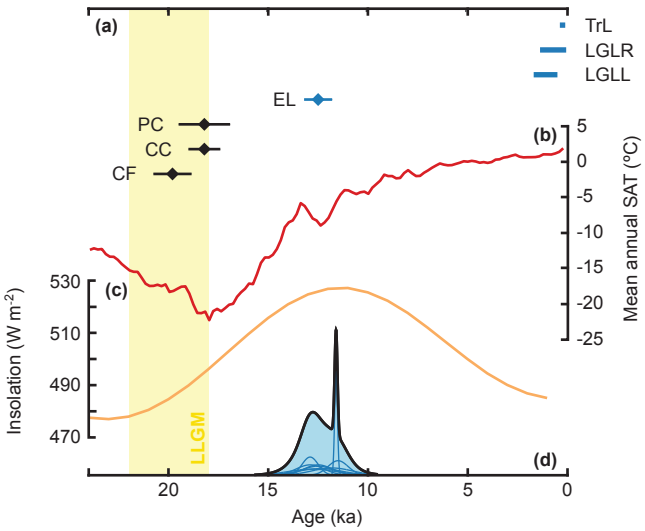

Fig. 5 - LGM, Deglacial, and Holocene- Diamonds indicate moraine ages. (a) Blue diamonds are ages from this study. Blue bars represent the age range for late-Holocene samples. TrL = Triangle Lake, LGLL = Little Glacier Lake left lateral moraine, LGLO = Little Glacier Lake right lateral moraine. Black diamonds are ages from Licciardi & Pierce (2018). PC = Pine Creek moraine, CC = Crandall Creek, CF = Clarks Fork. (b) Red line is mean annual surface temperature for our study area taken from Osman et al. (2021). (c) Orange line is mean annual insolation for 45° N. (d) Bottom probability distribution shaded in blue is for the compilation of western U.S. Younger Dryas moraines taken from Marcott et al. (2019), Licciardi and Pierce (2018), and the Emerald Lake moraine from this study. Yellow box highlights the timing of the local LGM from 22 ka to 18 ka.

5.2 The Younger Dryas

Presence of the Emerald Lake moraine shows the location of the glacier in the latest Pleistocene, older than the previously proposed Neoglacial age (Graf, 1971), and marks a pinning point of glaciation during retreat from the LGM limits. Additionally, these data contribute to a growing data set of western U.S. moraine ages supporting a regional response of mountain glaciers to the Younger Dryas (YD; Marcott et al., 2019),

The Emerald Lake moraine marks the first location of the glacier margin in the Upper Valley ~27 km upvalley from the LGM position. Presence of the moraine indicates stillstand or readvance of the glacier during the latest Pleistocene, perhaps in response to YD cooling (12.9 – 11.7 ka; Davis et al., 2009; Gosse et al., 1995). Geochronologic studies from glaciers in additional western U.S. mountain ranges identify similar glacier responses to YD cooling (Gosse et al., 1995; Licciardi and Pierce, 2008; Marcott et al., 2019) while other paleoclimate proxies identify a YD signal in the region (Mix et al., 1999; Praetorius et al., 2020, 2015; Vacco et al., 2005). However, uncertainty of the exposure ages, and differences in production rate calculations, prevent conclusively attributing formation of the Emerald Lake moraine to the early- or later-portions of the YD stadial. Two potential scenarios arise: (1) deposition

of the moraine early in the YD cooling with glacier retreat continuing throughout the stadial, and (2) deposition in response to YD cooling and retreat following abrupt warming at the end of the YD.

The age of the Emerald Lake moraine places retreat of the glacier from this location 12.5 ± 0.7 ka with glacial stabilization occurring prior to this time (Fig. 5). Morainal deposits near the Lake Solitude cirque lip in the nearby Teton Range (~175 km to the south) are dated to 12.9 ± 0.7 ka (Licciardi and Pierce, 2008; recalculated in Licciardi and Pierce, 2018). Together the ages of the Emerald Lake and Lake Solitude moraines imply a glacier response to the YD cooling with retreat during, or after, the stadial. A compilation of YD-age deposits from the western U.S. (Marcott et al., 2019), calculated using the PPT production rate and LSDn scaling scheme, highlight 9 separate moraine exposure ages (including the Emerald Lake and Lake Solitude moraines) between 12.9 ± 0.7 ka (Licciardi and Pierce, 2008) and 11.5 ± 0.5 ka (Marcott et al., 2019). Mean age and standard deviation of these moraines are 12.3 ± 0.6 ka, while probability density indicates a higher peak earlier in the stadial (12.8 ka). All moraines in the compilation exist between 37-45º N and above 2765 m elevation. Taken together, these exposure ages suggest a regional glacial response to the YD stadial, with variability in timing of morainal abandonment– potentially driven by differences in precipitation patterns (Lora and Ibarra, 2019), atmospheric lapse rate (Loomis et al., 2017; Zhang et al., 2019), or topographic control (Barr and Spagnolo, 2015). However, multi-centennial scale uncertainties within each age prevent conclusive attribution of moraines to early or late periods of the YD.

Age of the Emerald Lake moraine calculated using the TL production rate (11.6 ± 0.6 ka) indicates retreat of the glacier later in the YD. Even with consideration of age uncertainty, the reported exposure age highlights moraine abandonment ~700 years after the onset of the YD stadial at a minimum (Fig. 5). As such, the glacier potentially stabilized in response to abruptly suppressed temperatures, maintained its position for > 700 years, and retreated as temperatures recovered at the end of the stadial. However, the deflated nature of the Emerald Lake moraine lies in contrast to the much younger Triangle and Frosty Lake moraines, as well as to the older LGM moraines found at Clarks Fork and Black Butte. Similar low-profile morainal deposits associated with mountain glaciation are attributed to high-frequency glacier length variability during deglaciation (Barth et al., 2018). Therefore, the subdued profile of the Emerald Lake moraine suggests any period of stagnation was short-lived and/or characterized by low depositional rates. Any forcing of this response had minor impact in the overall trend of glacier retreat.

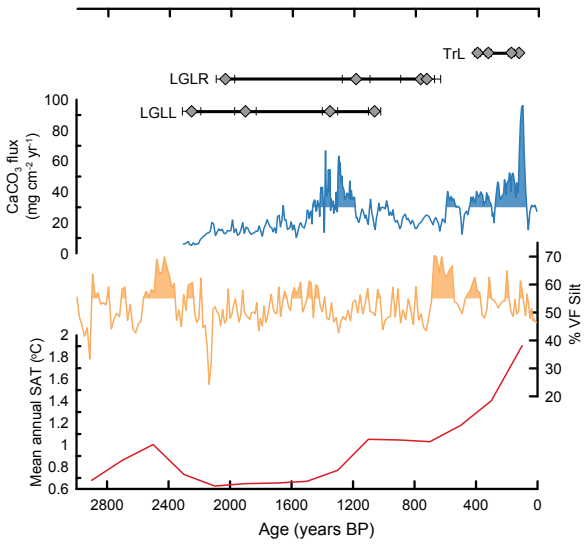

Fig. 6 - Neoglacial – (a) Ages for the late-Holocene moraines from this study adjusted to reflect years before present. Black lines indicate age range for all samples within a moraine population. Gray diamonds are individual ^{10}Be ages with 1-sigma uncertainty. (b) Blue line shows the $CaCO_3$ flux from Harrison Lake in Glacier National Park (Munroe et al., 2012). Shaded areas indicate greater than mean values for the time series and interpreted as increased glacial activity in the original study. (c) Orange line shows the percent very fine silt fraction from Cracker Lake in Glacier National Park (Munroe et al., 2012). Shaded areas indicate greater than mean values and increased glacial activity. (d) Red line is the mean annual surface temperature for our study region taken from Osman et al. (2021).

5.3 Constraints on Neoglaciation and the Little Ice Age

Ages from the Little Glacier Lake and Triangle Lake moraines indicate Upper Valley glacier activity within the late Holocene (Fig. 6). Glaciation in the western U.S. is suggested to have reached a minimum in the early Holocene due to high Northern Hemisphere summer insolation (Porter and Denton, 1967). Multiple archives across the northern hemisphere highlight a readvance of glaciers in the later Holocene (Munroe et al., 2012; Porter and Denton, 1967; Reyes et al., 2006; Solomina et al., 2015) due to declining summer temperatures (Marcott et al., 2013; McKay et al., 2018). Late-Holocene, Neoglacial deposits are found in numerous mountain ranges across the western U.S. and Canada, Greenland, Europe, and Asia (Briner and Porter, 2018; Graf, 1971; Marcott et al., 2019; Munroe et al., 2012; Reyes et al., 2006; Solomina et al., 2015).

Surface exposure ages from boulders within the Little Glacier Lake moraines exhibit a broad range suggestive of geologic uncertainty. One possible explanation for the wide range of ages is some boulders contain accumulated nuclides from previous periods of exposure and are perhaps sourced from rock fall from the nearby cirque headwall and cliff faces. Based on geomorphological characteristics, including the bouldery nature and steep toe of the moraine, another possibility is that this moraine is the product of rock glaciation with lower rates of erosion less likely to remove previously accumulated nuclides from past periods of exposure. The sample population as a whole demonstrates a multi-modal distribution, which could be interpreted as numerous periods of glaciation. As such, we discuss here the range of ages and interpret them as a limiting range of deglaciation from the moraine and suggestive of glacial conditions prior to abandonment.

Age of the Little Glacier Lake moraines indicate conditions within the Upper Valley had become favorable for glacier activity by 2,250 ± 60 to 720 ± 50 years ago with glaciation likely occurring prior to this time (Fig. 6a). These data also imply that subsequent glaciation (e.g., LIA) did not exceed this boundary which therefore represents the maximum late-Holocene glacial extent. Based on geomorphic evidence and variability among exposure ages, we suggest that the Little Glacier Lake moraines represent rock glaciation and formed through transitional glacial and periglacial processes (Petersen et al., 2020). Therefore, continued and variable glacial-periglacial conditions for the Little Glacier Lake rock glacier is demonstrated by the full range of exposure ages until abandonment by 720 ± 50 yrs at the latest.

In nearby Glacier National Park, MT (~500 km north of the Beartooth Mountains) proglacial lake sediments are interpreted to indicate glacier fluctuations throughout the Holocene including phases of glacier advance 2,300 and 1,500 cal year BP and again after 700 cal year BP (Fig. 6; Munroe et al., 2012). Paleo-proxy reconstructions of temperature and precipitation for the region indicate lower than average temperatures and increased winter precipitation ~1,600-1,200 years ago with continued decreased temperatures ~700 years ago (Trouet et al., 2013; Viau et al., 2012). Together these various proxies of climate and glacier activity suggest climate conditions favorable for glaciation marked by small-scale glacier fluctuations and regional variability.

Continuation of climate/glacier variability recorded in ages of the Little Glacier Lake deposits and regional paleo-proxies culminated with the glaciation recorded in the Triangle Lake moraine. Morainal abandonment of the Triangle Lake glacier between 390 ± 20 and 120 ± 10 yrs ago marks the end of substantial moraine construction within the Upper Valley. Similarities between the Triangle Lake and the upvalley Frosty Lake moraine morphologies imply similar age and behavior of the two glaciers. Both moraines are large (>50 m relief) likely from either long duration of moraine construction at the boundary or high depositional rates. We suggest late-Holocene reactivation of the Triangle Lake glacier was synchronous with the onset of glaciation recorded in the Little Glacier Lake deposits as both responded to the same forcing. Unlike at Little Glacier Lake, the Triangle Lake glacier maintained its position and positive mass balance longer, thus constructing a more substantial moraine and staving off rock glaciation, which can occur as a periglacial feature (Giardino and Vitek, 1988; Knight et al., 2019).

A recent study of glaciers in New Zealand highlighted the inverse hemispheric relationship as those glaciers reached maximum lengths early in the Holocene and retreated ever since (Dowling et al., 2021). It is likely that glaciers and periglacial features in the higher elevations of the Beartooth Mountains reactivated in response to late-Holocene low NH insolation levels, and provide evidence of cooler, and more favorable, climates in the last half of the Holocene. Though proximal, differences in Little Glacier Lake and Triangle Lake glacier response to climate forcing could be driven by the influence of higher, and more shaded, headwalls surrounding the Triangle Lake glacier. Similar topographic scenarios have been shown to influence alpine glacier advances (Barr and Spagnolo, 2015). Taken together, the Little Glacier Lake and Triangle Lake exposure ages suggest reactivation of glaciers within the Upper Valley from their early Holocene minima during the Neoglaciation prior to 2,250 ± 60 yrs with deglaciation occurring as late as 120 ± 10 yrs. Exposure ages from the Little Glacier Lake deposits support regional studies suggestive of glacier fluctuations and climate variability throughout the Neoglaciation.

6 Conclusion

New ^{10}Be surface exposure ages from the Rock Creek drainage in the eastern Beartooth mountain range yield new insight into the timing of western U.S. glaciation. After likely retreating from the LGM limit between 22 ka and 18 ka, the glacier stabilized in the Upper Valley during the Younger Dryas stadial as evidenced by the Emerald Lake moraine (12.5 ± 0.7 ka). This age redefines the age of the deposit, which was initially suggested to be Neoglacial in age by Graf (1971), and fits a trend of previously assigned Neoglacial deposits being geochronologically constrained to latest Pleistocene and earliest Holocene glaciation (Marcott et al., 2019). Evidence of Neoglaciation is found within the Upper Valley in the presence of the Little Glacier Lake lateral moraines that yield a range of exposure ages between 2,250 ± 60 yrs and 1,060 ± 40 yrs, with continued glacial-periglacial rock glacier fluctuations occurring throughout the late Holocene between 2,030 ± 60 yrs and 720 ± 50 yrs. These deposits support evidence that climatic conditions within the western U.S. were favorable for glaciation at high elevations in the late Holocene (Marcott et al., 2019; Solomina et al., 2016). Glaciation continued within the Upper Valley until retreat of the Triangle Lake glacier between 390 ± 20 yrs and 120 ± 10 yrs, with only ephemeral glaciers and ice patches remaining today.

Data availability

Data from this study including those used in the figures are available in the Supplement.

Supplement link

The supplement related to this article is available online.

Author contributions

AMB: Conceptualization, Investigation, Writing – Original Draft, Visualization, Funding acquisition. EGC: Investigation, Writing – Review and Editing. CV: Investigation, Writing – Review and Editing. SAM: Conceptualization, Investigation, Writing – Review and Editing, Funding acquisition. JDS: Conceptualization, Investigation, Writing – Review and Editing. MWC: Investigation, Writing – Review and Editing.

Competing interests

The authors declare that they have no conflict of interest.

References

Balco, G., 2011. Contributions and unrealized potential contributions of cosmogenic-nuclide exposure dating to glacier chronology, 1990–2010. Quaternary Science Reviews 30, 3–27. https://doi.org/10.1016/j.quascirev.2010.11.003

Balco, G., Stone, J.O., Lifton, N.A., Dunai, T.J., 2008. A complete and easily accessible means of calculating surface exposure ages or erosion rates from 10Be and 26Al measurements. Quaternary Geochronology 3, 174–195. https://doi.org/10.1016/j.quageo.2007.12.001

Ballard, G.A., 1976. Evidence to suggest catastrophic flooding of Clarks Fork of the Yellowstone River, northeastern Wyoming (M.S.). University of Utah.

Barr, I.D., Spagnolo, M., 2015. Glacial cirques as palaeoenvironmental indicators: Their potential and limitations. Earth-Science Reviews 151, 48–78. https://doi.org/10.1016/j.earscirev.2015.10.004

Barth, A.M., Clark, P.U., Clark, J., Roe, G.H., Marcott, S.A., McCabe, A.M., Caffee, M.W., He, F., Cuzzone, J.K., Dunlop, P., 2018. Persistent millennial-scale glacier fluctuations in Ireland between 24 ka and 10 ka. Geology 46, 151–154. https://doi.org/10.1130/G39796.1

Bevan, A., 1923. Summary of the Geology of the Beartooth Mountains, Montana. The Journal of Geology 31, 441–465. https://doi.org/10.1086/623038

Bolch, T., 2007. Climate change and glacier retreat in northern Tien Shan (Kazakhstan/Kyrgyzstan) using remote sensing data. Global and Planetary Change 56, 1–12. https://doi.org/10.1016/j.gloplacha.2006.07.009

Braumann, S.M., Schaefer, J.M., Neuhuber, S.M., Reitner, J.M., Lüthgens, C., Fiebig, M., 2020. Holocene glacier change in the Silvretta Massif (Austrian Alps) constrained by a new 10Be chronology, historical records and modern observations. Quaternary Science Reviews 245, 106493. https://doi.org/10.1016/j.quascirev.2020.106493

Briner, J.P., Porter, S.C., 2018. Neoglaciation in the American Cordilleras, in: Encyclopedia of Quaternary Science. Elsevier, pp. 1133–1142. https://doi.org/10.1016/B0-444-52747-8/00137-X

Catania, G.A., Stearns, L.A., Sutherland, D.A., Fried, M.J., Bartholomaus, T.C., Morlighem, M., Shroyer, E., Nash, J., 2018. Geometric Controls on Tidewater Glacier Retreat in Central Western Greenland. J. Geophys. Res. Earth Surf. 123, 2024–2038. https://doi.org/10.1029/2017JF004499

Clark, P.U., Dyke, A.S., Shakun, J.D., Carlson, A.E., Clark, J., Wohlfarth, B., Mitrovica, J.X., Hostetler, S.W., McCabe, A.M., 2009. The Last Glacial Maximum. Science 325, 710–4. https://doi.org/10.1126/science.1172873

Corbett, L.B., Bierman, P.R., Rood, D.H., 2016. An approach for optimizing in situ cosmogenic 10Be sample preparation. Quaternary Geochronology 33, 24–34. https://doi.org/10.1016/j.quageo.2016.02.001

Davis, P., 1988. Holocene glacier fluctuations in the American Cordillera. Quaternary Science Reviews 7, 129–157. https://doi.org/10.1016/0277-3791(88)90003-0

Davis, P.T., Menounos, B., Osborn, G., 2009. Holocene and latest Pleistocene alpine glacier fluctuations: a global perspective. Quaternary Science Reviews 28, 2021–2033. https://doi.org/10.1016/j.quascirev.2009.05.020

Dowling, L., Eaves, S., Norton, K., Mackintosh, A., Anderson, B., Hidy, A., Lorrey, A., Vargo, L., Ryan, M., Tims, S., 2021. Local summer insolation and greenhouse gas forcing drove warming and glacier retreat in New Zealand during the Holocene. Quaternary Science Reviews 266, 107068. https://doi.org/10.1016/j.quascirev.2021.107068

Dunai, T.J., 2010. Cosmogenic Nuclides: Principles, Concepts and Applications in the Earth Surface Sciences. Cambridge University Press, United Kingdom.

Giardino, J.R., Vitek, J.D., 1988. The significance of rock glaciers in the glacial-periglacial landscape continuum. J. Quaternary Sci. 3, 97–103. https://doi.org/10.1002/jqs.3390030111

Gillespie, A.R., Bierman, P.R., 1995. Precision of terrestrial exposure ages and erosion rates estimated from analysis of cosmogenic isotopes produced in situ. J. Geophys. Res. 100, 24637–24649. https://doi.org/10.1029/95JB02911

Gosse, J.C., Evenson, E.B., Klein, J., Lawn, B., Middleton, R., 1995. Precise cosmogenic 10Be measurements in western North America: Support for a global Younger Dryas cooling event. Geology 23, 877–880.

Gosse, J.C., Phillips, F.M., 2001. Terrestrial in situ cosmogenic nuclides: theory and application. Quaternary Science Reviews 20, 1475–1560.

Graf, W.L., 1971. Quantitative Analysis of Pinedale Landforms, Beartooth Mountains, Montana and Wyoming. Arctic and Alpine Research 3, 253. https://doi.org/10.2307/1550197

Hugonnet, R., McNabb, R., Berthier, E., Menounos, B., Nuth, C., Girod, L., Farinotti, D., Huss, M., Dussaillant, I., Brun, F., Kääb, A., 2021. Accelerated global glacier mass loss in the early twenty-first century. Nature 592, 726–731. https://doi.org/10.1038/s41586-021-03436-z

Knight, J., Harrison, S., Jones, D.B., 2019. Rock glaciers and the geomorphological evolution of deglacierizing mountains. Geomorphology 324, 14–24. https://doi.org/10.1016/j.geomorph.2018.09.020

Kohl, C.P., Nishiizumi, K., 1992. Chemical isolation of quartz for measurement of in-situ-produced cosmogenic nuclides. Geochimica et Cosmochimica Acta 56, 3583–3587.

Laabs, B.J.C., Licciardi, J.M., Leonard, E.M., Munroe, J.S., Marchetti, D.W., 2020. Updated cosmogenic chronologies of Pleistocene mountain glaciation in the western United States and associated paleoclimate inferences. Quaternary Science Reviews 242, 106427. https://doi.org/10.1016/j.quascirev.2020.106427

Licciardi, J., 2000. Alpine Glacier and Pluvial Lake Records of Late Pleistocene Climate Variability in the Western United States (Dissertation). Oregon State University.

Licciardi, J.M., Pierce, K.L., 2018. History and dynamics of the Greater Yellowstone Glacial System during the last two glaciations. Quaternary Science Reviews 200, 1–33. https://doi.org/10.1016/j.quascirev.2018.08.027

Licciardi, J.M., Pierce, K.L., 2008. Cosmogenic exposure-age chronologies of Pinedale and Bull Lake glaciations in greater Yellowstone and the Teton Range, USA. Quaternary Science Reviews 27, 814–831. https://doi.org/10.1016/j.quascirev.2007.12.005

Lifton, N., Caffee, M., Finkel, R., Marrero, S., Nishiizumi, K., Phillips, F.M., Goehring, B., Gosse, J., Stone, J., Schaefer, J., Theriault, B., Jull, A.J.T., Fifield, K., 2015. In situ cosmogenic nuclide production rate calibration for the CRONUS-Earth project from Lake Bonneville, Utah, shoreline features. Quaternary Geochronology 26, 56–69. https://doi.org/10.1016/j.quageo.2014.11.002

Lifton, N., Sato, T., Dunai, T.J., 2014. Scaling in situ cosmogenic nuclide production rates using analytical approximations to atmospheric cosmic-ray fluxes. Earth and Planetary Science Letters 386, 149–160. https://doi.org/10.1016/j.epsl.2013.10.052

Loomis, S.E., Russell, J.M., Verschuren, D., Morrill, C., De Cort, G., Sinninghe Damsté, J.S., Olago, D., Eggermont, H., Street-Perrott, F.A., Kelly, M.A., 2017. The tropical lapse rate steepened during the Last Glacial Maximum. Sci. Adv. 3, e1600815. https://doi.org/10.1126/sciadv.1600815

Lora, J.M., Ibarra, D.E., 2019. The North American hydrologic cycle through the last deglaciation. Quaternary Science Reviews 226, 105991. https://doi.org/10.1016/j.quascirev.2019.105991

Lora, J.M., Mitchell, J.L., Risi, C., Tripati, A.E., 2017. North Pacific atmospheric rivers and their influence on western North America at the Last Glacial Maximum. Geophys. Res. Lett. 44, 1051–1059. https://doi.org/10.1002/2016GL071541

Manabe, S., Broccoli, A.J., 1985. The influence of continental ice sheets on the climate of an ice age. J. Geophys. Res. 90, 2167. https://doi.org/10.1029/JD090iD01p02167

Marcott, S.A., 2011. Late Pleistocene and Holocene Glacier and Climate Change. Oregon State University.

Marcott, S.A., Bauska, T.K., Buizert, C., Steig, E.J., Rosen, J.L., Cuffey, K.M., Fudge, T.J., Severinghaus, J.P., Ahn, J., Kalk, M.L., McConnell, J.R., Sowers, T., Taylor, K.C., White, J.W., Brook, E.J., 2014. Centennial-scale changes in the global carbon cycle during the last deglaciation. Nature 514, 616–9. https://doi.org/10.1038/nature13799

Marcott, S.A., Clark, P.U., Shakun, J.D., Brook, E.J., Davis, P.T., Caffee, M.W., 2019. 10Be age constraints on latest Pleistocene and Holocene cirque glaciation across the western United States. npj Clim Atmos Sci 2, 5. https://doi.org/10.1038/s41612-019-0062-z

Marcott, S.A., Shakun, J.D., Clark, P.U., Mix, A.C., 2013. A reconstruction of regional and global temperature for the past 11,300 years. Science 339, 1198–201. https://doi.org/10.1126/science.1228026

McKay, N.P., Kaufman, D.S., Routson, C.C., Erb, M.P., Zander, P.D., 2018. The Onset and Rate of Holocene Neoglacial Cooling in the Arctic. Geophys. Res. Lett. 45, 12,487-12,496. https://doi.org/10.1029/2018GL079773

Mix, A.C., Lund, D.C., Pisias, N.G., Bodén, P., Bornmalm, L., Lyle, M., Pike, J., 1999. Rapid climate oscillations in the Northeast Pacific during the last deglaciation reflect Northern and Southern Hemisphere sources, in: Rapid Climate Oscillations in the Northeast Pacific during the Last Deglaciation Reflect Northern and Southern Hemisphere Sources, AGU Monograph. American Geophysical Union, Washington, D. C., pp. 127–148.

Montgomery, C.W., Lytwyn, J.N., 1984. Rb-Sr Systematics and Ages of Principal Precambrian Lithologies in the South Snowy Block, Beartooth Mountains. The Journal of Geology 92, 103–112. https://doi.org/10.1086/628837

Munroe, J.S., Crocker, T.A., Giesche, A.M., Rahlson, L.E., Duran, L.T., Bigl, M.F., Laabs, B.J.C., 2012. A lacustrine-based Neoglacial record for Glacier National Park, Montana, USA. Quaternary Science Reviews 53, 39–54. https://doi.org/10.1016/j.quascirev.2012.08.005

Nishiizumi, K., Imamura, M., Caffee, M.W., Southon, J.R., Finkel, R.C., McAninch, J., 2007. Absolute calibration of 10Be AMS standards. Nuclear Instruments and Methods in Physics Research Section B: Beam Interactions with Materials and Atoms 258, 403–413. https://doi.org/10.1016/j.nimb.2007.01.297

Osman, M.B., Tierney, J.E., Zhu, J., Tardif, R., Hakim, G.J., King, J., Poulsen, C.J., 2021. Globally resolved surface temperatures since the Last Glacial Maximum. Nature 599, 239–244. https://doi.org/10.1038/s41586-021-03984-4

Petersen, E.I., Levy, J.S., Holt, J.W., Stuurman, C.M., 2020. New insights into ice accumulation at Galena Creek Rock Glacier from radar imaging of its internal structure. J. Glaciol. 66, 1–10. https://doi.org/10.1017/jog.2019.67

Porter, S.C., Denton, G.H., 1967. Chronology of neoglaciation in the North American Cordillera. American Journal of Science 265, 177–210.

Praetorius, S.K., Condron, A., Mix, A.C., Walczak, M.H., McKay, J.L., Du, J., 2020. The role of Northeast Pacific meltwater events in deglacial climate change. Sci. Adv. 6, eaay2915. https://doi.org/10.1126/sciadv.aay2915

Praetorius, S.K., Mix, A.C., Walczak, M.H., Wolhowe, M.D., Addison, J.A., Prahl, F.G., 2015. North Pacific deglacial hypoxic events linked to abrupt ocean warming. Nature 527, 362–6. https://doi.org/10.1038/nature15753

Putkonen, J., Connolly, J., Orloff, T., 2008. Landscape evolution degrades the geologic signature of past glaciations. Geomorphology 97, 208–217. https://doi.org/10.1016/j.geomorph.2007.02.043

Reyes, A.V., Wiles, G.C., Smith, D.J., Barclay, D.J., Allen, S., Jackson, S., Larocque, S., Laxton, S., Lewis, D., Calkin, P.E., Clague, J.J., 2006. Expansion of alpine glaciers in Pacific North America in the first millennium A.D. Geol 34, 57. https://doi.org/10.1130/G21902.1

Shakun, J.D., Clark, P.U., He, F., Lifton, N.A., Liu, Z., Otto-Bliesner, B.L., 2015. Regional and global forcing of glacier retreat during the last deglaciation. Nat Commun 6, 8059. https://doi.org/10.1038/ncomms9059

Solomina, O.N., Bradley, R.S., Hodgson, D.A., Ivy-Ochs, S., Jomelli, V., Mackintosh, A.N., Nesje, A., Owen, L.A., Wanner, H., Wiles, G.C., Young, N.E., 2015. Holocene glacier fluctuations. Quaternary Science Reviews 111, 9–34. https://doi.org/10.1016/j.quascirev.2014.11.018

Solomina, O.N., Bradley, R.S., Jomelli, V., Geirsdottir, A., Kaufman, D.S., Koch, J., McKay, N.P., Masiokas, M., Miller, G., Nesje, A., Nicolussi, K., Owen, L.A., Putnam, A.E., Wanner, H., Wiles, G., Yang, B., 2016. Glacier fluctuations during the past 2000 years. Quaternary Science Reviews 149, 61–90. https://doi.org/10.1016/j.quascirev.2016.04.008

Sortor, R.N., 2022. Glacial chronologies of western North American mountain ranges from cosmogenic nuclide dating (PhD Dissertation). Tulane University.

Trouet, V., Diaz, H.F., Wahl, E.R., Viau, A.E., Graham, R., Graham, N., Cook, E.R., 2013. A 1500-year reconstruction of annual mean temperature for temperate North America on decadal-to-multidecadal time scales. Environmental Research Letters 8, 024008. https://doi.org/10.1088/1748-9326/8/2/024008

Vacco, D.A., Clark, P.U., Mix, A.C., Cheng, H., Edwards, R.L., 2005. A speleothem record of Younger Dryas cooling, Klamath Mountains, Oregon, USA. Quaternary Research 64, 249–256.

Van Gosen, B.S., Elliot, J.E., LaRock, E.J., du Bray, E.A., Carlson, R.R., Zientek, M.L., 2000. Generalized geologic map of the Absaroka-Beartooth study area, south-central Montana. https://doi.org/10.3133/mf2338

Viau, A.E., Ladd, M., Gajewski, K., 2012. The climate of North America during the past 2000years reconstructed from pollen data. Global and Planetary Change 84–85, 75–83. https://doi.org/10.1016/j.gloplacha.2011.09.010

Young, N.E., Briner, J.P., Leonard, E.M., Licciardi, J.M., Lee, K., 2011. Assessing climatic and nonclimatic forcing of Pinedale glaciation and deglaciation in the western United States. Geology 39, 171–174. https://doi.org/10.1130/g31527.1

Zhang, E., Chang, J., Shulmeister, J., Langdon, P., Sun, W., Cao, Y., Yang, X., Shen, J., 2019. Summer temperature fluctuations in Southwestern China during the end of the LGM and the last deglaciation. Earth and Planetary Science Letters 509, 78–87. https://doi.org/10.1016/j.epsl.2018.12.024